Geometries and Stabilities of the Carbon Clusters with the Rhodium Impurity: A Computational Investigation

Li-Chao Jia,[†] Run-Ning Zhao,[‡] Ju-Guang Han,*[,‡] Liu-Si Sheng,[‡] and Wei-Ping Cai[†]

Institute of Solid State Physics, The Chinese Academy of Sciences, Hefei 230031, People's Republic of China, National Synchrotron Radiation Laboratory, University of Science and Technology of China, Hefei 230026, People's Republic of China

Received: December 2, 2007; In Final Form: January 28, 2008

A density functional study of the RhC_n($n = 1-6$) clusters with different spin states has been carried out systematically by using the B3LYP/Lan2DZ method. The equilibrium geometries associated with total energies and natural populations of RhC_n ($n = 1-6$) clusters are calculated and presented. Stabilities and electronic properties are discussed in detail. The relative stabilities in term of the calculated fragmentation energies show that the lowest-energy RhC_n clusters with rhodium atom being located at terminal of carbon chain are the linear geometries and the ground states of the RhC_n clusters alternate between doublet (for *n*-odd members) and quartet (for *n*-even members) states. Furthermore, the calculated fragmentation energies of the RhC_n show strong even−odd alternations: the RhC_n clusters with an odd number of carbon atoms are more stable than those with an even number ones. In addition, we comment on the charge transfer and chemical bonding properties within the clusters.

1. Introduction

To understand a variety of chemical properties of carbon clusters (e.g., fullerene and nanotube carbon clusters), many experimental and theoretical investigations have been studied in the past decades.[1−3] Small carbon clusters were studied with great interest because they are intermediates in chemical vapor deposition of carbon clusters and can be exactly identified in interstellar and circumstellar media by radiowave or infrared spectroscopy in astrophysics.[4] In the interstellar medium, the reactivity of small carbon clusters shows their light reactivity because of the quasicollisionless conditions, and highly linear chains carbon clusters are observed. Furthermore, the discovery and successful preparation[3] of C_{60} and other fullerenes have spawned a new branch of chemistry.

Heteroatom-doped carbon clusters result in significant changes in the geometrical and electronic structures, which may eventually be used to elaborate new types of materials with interesting applications and novel properties. In this respect, it is very important to have some knowledge about the behavior of transition metal-doped carbon clusters. This will allow the identification of possible systematic trends that could help us understand the structure of these materials and get information that could be useful to make extrapolations for some properties. Much interest has been focused on nonmetallic and metallic carbide clusters, such as SC_n[5], SiC_n,[6] PC_n,[7] ClC_n[8], AlC_n,[9,10] MgC_n,[11,12] and CaC_n[13,14] clusters. Recently, these kinds of experimental studies have been extended to heavier transition metal carbon clusters combined with mass spectrometry, the ion drift tube technique, high-resolution optical spectroscopy, photoelectron spectroscopy, ESR spectroscopy for YC, NbC, PdC, and RhC etc.[15−24]

Surprisingly, there are few theoretical studies on the structures and stabilities of the transition metal doped carbon clusters. A theoretical study of the linear PbC_n clusters and the transition metal carbides of CrC_n, YC_n, LaC_n, NbC_n, and ScC_n[25−30] clusters have recently been investigated systemically. A number of carbides containing rhodium atoms, i.e., RhC,[31] RhN,[32] $RhCH_3$,[31] RhHCO,[34] and $Rh(CO_2)$,[34] have also been studied theoretically.

Although the diatomic RhC has been studied both experimentally and theoretically, to the best of our knowledge, no experimental or theoretical investigation on the RhC_n ($n = 1-6$) clusters has been reported. To reveal the unusual properties of the rhodium-doped carbon clusters, the aim of the studies reported here is to provide a detailed investigation of equilibrium geometries, charge-transfer properties, relative stabilities, fragmentation energies [$D(n, n-1)$], atomic averaged binding energies [$E_b(n)$], and HOMO−LUMO gaps of these RhC_n clusters. The analyzed results help us understand chemical and physical properties of the Rhodium doped carbon clusters.

2. Computational Details

All calculations were performed with the hybrid Becke (B3) exchange and the Lee, Yang and Parr (LYP) correlation (B3LYP) functionals in combination with the Los Alamos ECP D95V and double-ζ basis sets (LanL2DZ) as implemented in the Gaussian 98 code.[35−40] For each stationary point of the clusters, the stability is examined by calculating the harmonic vibrational frequencies. If an imaginary frequency is found, a relaxation along the coordinates of the imaginary vibrational mode is carried out until a true local minimum is reached. Therefore, the reported geometries and total energies for each stable cluster and its stable isomers correspond to local minima. However, as the number of isomers increases rapidly with the cluster size, it is very difficult to determine the global minimum simply according to the calculated energies of the isomers. To find the stable RhC_n ($n = 1-6$) geometries, we considered first some previous theoretical or experimental geometries that are

* To whom correspondence should be addressed. E-mail: jghan@ustc.edu.cn. Fax: 86-551-5141078.
† The Chinese Academy of Sciences.
‡ University of Science and Technology of China.

10.1021/jp711380x CCC: $40.75
Published on Web 04/08/2008

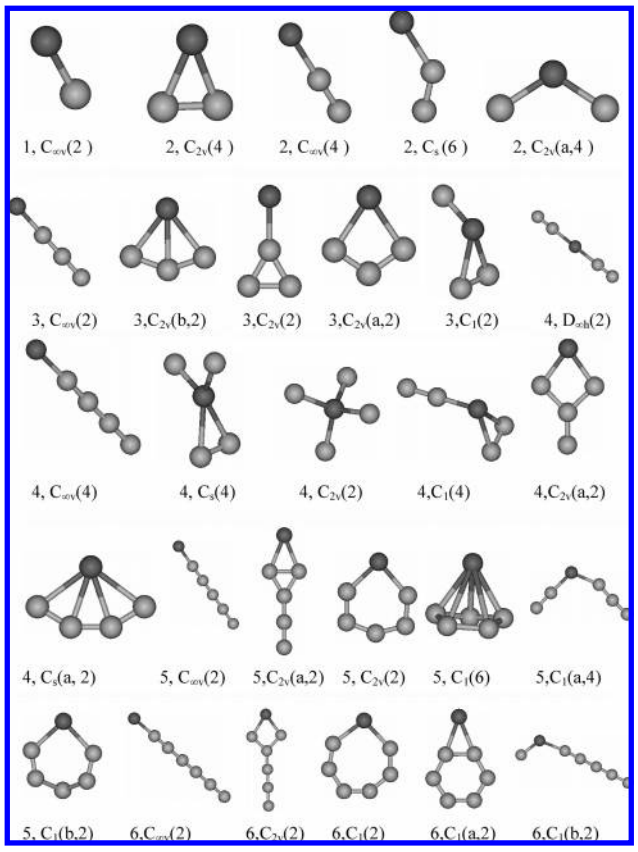

Figure 1. Equilibrium geometries of the RhC_n ($n = 1-6$) clusters. For example, the $C_1(2)$ above represents the doublet state with C_1 symmetry.

available, we varied the structure starting from high-symmetry structure and reducing the symmetry. The spin of the RhC_n clusters were restricted to $S = 1/2$, 3/2, and 5/2. The spin contamination is zero and can be neglected.

3. Results and Discussion

The calculated results of bond lengths and bond angles, together with total energies, are listed in Table 1; Milliken atomic net populations are listed in Table 2. Natural populations and natural electron configurations of the RhC_n ($n = 1-6$) clusters are listed in Table 3, whereas the equilibrium geometries of RhC_n ($n = 1-6$) are displayed in Figure 1.

3.1. Geometry and Stability. To check the reliability of our calculations, we calculated the bond lengths of C_2 and Rh_2 dimers at the UB3LYP/LanL2DZ level. The calculated results show that the C−C bond length of C_2 dimer is 1.281 Å, which is in good agreement with those of B3LYP/ccp-VDZ(1.262 Å);[41] and that the Rh−Rh bond length (2.321 Å) corresponds to the previous results of the UHF/SHIM−SU method[42] with relativistic core potential (2.283 Å). On the basis of the tests above, the B3LYP/LANL2DZ method is believed to yield an adequate description of the bonding properties of C and Rh atoms in small molecular units.

3.1.1. RhC. The equilibrium geometry of the RhC cluster with $C_{\infty v}$ symmetry is optimized at the (U)B3LYP/LanL2DZ level (Figure 1). The Rh−C bond length depends on spin state and is elongated as spin increases monotonically. The total energies of RhC cluster are increased apparently as spin increases (Table 1). So the doublet RhC cluster is obviously the lowest-energy isomer and the ground state, and the corresponding electronic state is $^2\Sigma$. This feature is in good agreement with an available calculated result for RhC[42] and is similar to those for TaC,[43] VC,[24] and CoC;[44] however, it differs from results for MC (M = Sc, Nb, Al, and Na) clusters.[45−48,9]

The calculated Rh−C distance for the ground state RhC (1.669 Å) is also in good agreement with the previous theoretical results of Skaarup et al. (1.65 Å)[49] and the experimental value given by Norman et al.[50] (1.655 Å); however, it is slightly shorter than the previous calculated datum at the UHF/RECP level.[34] The frequency of the ground state is calculated to be 1057.8 cm^{-1}, comparson with an available experimental result (1000 ± 60 cm^{-1}) is made.[22]

3.1.2. RhC_2. Five RhC_2 isomers with C_s, $D_{\infty h}$, C_{2v}, C_{2v}(a), and $C_{\infty v}$ symmetries were considered. The linear $D_{\infty h}$ geometry is proved to be an unstable structure while the C_{2v} and C_{2v}(a) clusters as well as the linear $C_{\infty v}$ with different spin states are found to be stable geometries. As seen from the Table 1, the bond lengths and the total energies of the Rh-capped C_{2v} isomer have an evident correlation with the spin; the Rh−C bond length and the total energies increase monotonical as spin S goes from $S = 1/2$, to 3/2, and to 5/2, resulting in the weakness of the Rh−C bond interaction and the stability of C_{2v} isomer. Like the C_{2v} isomer, the Rh−C bond length and the bond angle ∠CRhC in the C_{2v}(a) isomer are increased monotonously with the spin going from $S = 1/2$, to 3/2, and to 5/2. The total energy of the quartet C_{2v}(a) structure, however, is lower than those of the doublet and sextet isomers. The Rh-terminated linear $C_{\infty v}$ isomer has similar feature to that of the C_{2v}(a) isomer; The total energy of the quartet isomer is the lowest one with the Rh−C and C−C bond lengths being the smallest ones. The bent C_s structure is a distortion of the Rh-capped C_{2v} isomer, but the geometry optimization of the doublet and quartet C_s isomers fail to be converged. The total energy of the sextet C_s isomer is higher than those of the other isomers.

On the basis of the calculated total energies, it is confirmed that the linear quartet $C_{\infty v}$ geometry with electronic state of $^4\Sigma$ is the lowest-energy isomer and is consequently selected as the ground state. This finding is different from those for the most stable doublet LaC_2,[28] NaC_2,[48] ScC_2,[51] and YC_2[27] isomers.

3.1.3. RhC_3. The RhC_3 clusters with C_2v, Cs, C_1, and the linear $C_{\infty v}$ isomers are taken into account. All of them are considered as ground-state candidates. The calculated results reveal that the scooplike C_1 isomer has higher total energy and cannot be competitive with the other isomers in stability. Exchanging the location of the Rh and the apex C atom results in a planar geometry: the three carbon atoms form an equilateral triangle and the Rh atom bonds to one of the carbon atoms, which we call the kitelike C_{2v} isomer. The calculated results prove that the kite-like C_{2v} geometry is a stable structure. From the Table 1, it can be seen that the total energy and the C−C bond length of the kitelike quartet C_{2v} structure are lower than those of the doublet and sextet states, thus the kitelike quartet C_{2v} geometry with electronic state of $^4B_2$ is the most stable structure.

Guided by the previous theoretical results on the YC_3[27] and LaC_3[28] clusters, two planar C_{2v}(a) and C_{2v}(b) isomers were considered. One is a ringlike C_{2v}(a) structure in which the Rh atom is inserted into the C_n ring, the other is a fanlike C_{2v}(b) structure with the Rh atom bonding to three carbon atoms. For these two isomers, the total energy increases monotonically as spin varies from S=1/2, to 3/2, and to 5/2. The calculated results indicate that the total energy of the doublet C_{2v} (a) isomer with electronic state of $^2A_1$ is slightly lower by about 0.005 hartree than that of the doublet C_{2v}(b) isomer with electronic state of $^2B_1$. The linear $C\infty v$ RhC_3 isomer was also optimized. The

TABLE 1: Geometries, Total Energies, and Electronic States of RhC_n ($n = 1-6$) Clusters

cluster	symmetry	spin	electronic state	R1[a] (Å)	R2[b] (Å)	α[c]	E_b[d] (Hartree)
RhC	$C_{\infty v}$	1/2	$^2\Sigma$	1.669			**−147.4691**
		3/2	$^4\Sigma$	1.798			−147.4149
		5/2	$^6\Sigma$	2.035			−147.3484
RhC_2	$C_{\infty v}$	1/2	$^2B_1$	1.916	1.350	180.00	−185.4438
		3/2	$^4B_1$	1.812	1.341	180.00	**−185.4871**
		5/2	$^6B_1$	1.846	1.521	180.00	−185.3575
	C_{2v}	1/2	$^2B_1$	1.933	1.390	42.34	−185.4759
		3/2	$^4B_1$	2.038	1.357	39.44	−185.4754
		5/2	$^6A_1$	2.041	1.526	43.91	−185.3405
	C_{2v}(a)	1/2	$^2B_2$	1.780		103.21	−185.4126
		3/2	$^4A_2$	1.789		111.98	−185.4133
		5/2	$^6B_2$	1.891		166.10	−185.3464
	C_s	5/2	$^6A''$	1.949	1.359	137.79	−185.4009
RhC_3	$C_{\infty v}$	1/2	$^2\Sigma$	1.781	1.307		**−223.5922**
		3/2	$^4\Sigma$	1.882	1.295		−223.4702
		5/2	$^6\Sigma$	2.022	1.291		−223.4692
	C_{2v}	1/2	$^2B_2$	1.868	1.415		−223.5165
		3/2	$^4B_2$	1.912	1.411		−223.5199
		5/2	$^6A_1$	2.002	1.450		−223.3965
	C_{2v}(a)	1/2	$^2A_1$	2.083	1.357	74.92	−223.5553
		3/2	$^4B_1$	2.212	1.341	67.86	−223.4919
		5/2	$^6A_1$	1.993	1.431	68.84	−223.4360
	C_{2v}(b)	1/2	$^2B_1$	2.113	1.365	75.65	−223.5503
		3/2	$^4B_1$	1.927	1.454	76.06	−223.4811
		5/2	$^6B_1$	1.992	1.430	68.42	−223.4360
	C_1	1/2	^2A	2.207	1.318	116.17	−223.4940
		3/2	^4A	1.919	1.312	108.32	−223.4623
		5/2	^6A	1.813	1.353	107.04	−223.4049
RhC_4	$C_{\infty v}$	1/2	$^2\Sigma$	1.915	1.302		−261.6061
		3/2	$^4\Sigma$	1.825	1.298		**−261.6369**
		5/2	$^6\Sigma$	1.906	1.279		−261.5366
	C_{2v}	1/2	$^2A_1$	1.869		110.49	−261.2672
		3/2	$^4B_2$	1.860		112.35	−261.2574
	C_{2v}(a)	1/2	$^2A_1$	1.879	1.335	99.85	−261.5292
		3/2	$^4A_2$	1.994	1.360	127.32	−261.5233
		5/2	$^6B_1$	1.930	1.410	136.17	−261.4551
	C_s	3/2	$^4A''$	1.908	1.317	93.44	−261.4015
		5/2	$^6A''$	1.824	1.390	119.92	−261.3694
	C_s(a)	1/2	$^2A''$	2.153	1.327	106.72	−261.5960
		3/2	$^4A''$	2.228	1.311	101.31	−261.5937
		5/2	$^6A''$	1.949	1.302	119.92	−261.5615
	C_1	1/2		1.808	1.343	110.35	−261.4993
		3/2		1.814	1.337	106.93	−261.5042
		5/2		1.908	1.320	154.44	−261.4751
	$D_{\infty h}$	1/2	$^2\Sigma$	1.977	1.283		−261.4086
		5/2	$^6\Sigma$	2.069	1.339		−261.3578
RhC_5	$C_{\infty v}$	1/2	$^2\Sigma$	1.793	1.284		**−299.7326**
		3/2	$^4\Sigma$	1.970	1.271		−299.6831
		5/2	$^6\Sigma$	2.096	1.265		−299.6030
	C_{2v}	1/2	$^2B_2$	1.912	1.327	86.25	−299.6744
		5/2	$^6A_1$	2.158	1.378	120.38	−299.6061
	C_{2v}(a)	1/2	$^2A_1$	1.994	1.298		−299.6278
		5/2	$^6B_2$	2.041	1.357		−299.4945
	C_1	1/2		2.163	1.429	69.55	−299.5063
		5/2		2.166	1.399	60.53	−299.5252
	C_1(a)	1/2		1.797	1.305	97.05	−299.6234
		3/2		1.883	1.309	115.50	−299.5994
		5/2		1.905	1.323	109.70	−299.5315
	C_1(b)	1/2		1.912	1.327	86.26	−299.6746
		3/2		2.017	1.372	89.81	−299.6417
		5/2		2.165	1.377	116.37	−299.6075
RhC_6	$C_{\infty V}$	1/2	$^2\Sigma$	1.871	1.259		−337.7612
		3/2	$^4\Sigma$	1.824	1.297		**−337.7853**
		5/2	$^6\Sigma$	1.919	1.312		−337.7082
	C_{2v}	1/2	$^2A_1$	1.885	1.296	70.139	−337.6796
		3/2	$^4A_2$	2.008	1.291	45.053	−337.6754
		5/2	$^6B_1$	1.942	1.284	59.637	−337.6162
	C_1	1/2	^2A	1.914	1.311	102.60	−337.7488
		3/2	^4A	1.939	1.292	95.76	−337.7487
		5/2	$^6A_2$	1.997	1.433	91.75	−337.7167
	C_1(a)	1/2		2.009	1.317	42.27	−337.7374
		3/2		2.019	1.308	40.66	−337.7004
		5/2		2.005	1.329	40.80	−337.6485
	C_1(b)	1/2		1.661	1.294	115.59	−337.7218
		3/2		1.766	1.295	109.97	−337.6850
		5/2		1.750	1.311	110.09	−337.6345

[a] R1 denote the shortest Rh−C bond lengths. [b] R2 denotes the shortest C−C bond length. [c] α denotes the bond angle of C−Rh−C. [d] E_b represents the total energy of RhC_n clusters.

TABLE 2: Mulliken Atomic Net Populations of RhC_n (n = 1−6) Clusters at the B3LYP Level Employing LanL2DZ Basis Sets

cluster	symmetry	spin	Rh	C_1	C_3	C_5
RhC	$C_{\infty v}$	1/2	0.0051			
RhC_2	$C_{\infty v}$	3/2	0.3401	−0.2381		
RhC_3	$C_{\infty v}$	1/2	0.2095	0.0372	0.0390	
RhC_4	$C_{\infty v}$	3/2	0.3097	−0.1768	−0.2545	
RhC_5	$C_{\infty v}$	1/2	0.2155	−0.1023	0.1546	−0.0076
RhC_6	$C_{\infty v}$	3/2	0.2856	−0.2058	0.0226	−0.2869

optimized results show that the $C\infty v$ RhC_3 cluster has a preference for the low spin state.

For the calculated total energies of the RhC_3 clusters described above, we calculated that the doublet $C\infty v$ isomer is the most stable structure; the RhC_3 ($C\infty v$, S=1/2) is selected as the ground state with electronic state being $^2\Sigma$. The linear ground state for the RhC_3 cluster is similar to the geometries of the AlC_3[52], NaC_3[53] and PdC_3[25] clusters. However, it significantly differs from those of transition metal carbides, such as LaC_3[28], NbC_3[29], YC_3[27], and ScC_3[30].

3.1.4. RhC_4. The RhC_4 clusters with $C_{\infty v}$, $D_{\infty h}$, and C_{3v} symmetries were selected as the initial geometries to be optimized. The linear $C_{\infty v}$ RhC_4 isomer with the Rh atom localized at the terminal was obtained by adding one C atom to the most stable RhC_3 cluster and optimizing to obtain a stable structure. The linear $D_{\infty h}$ geometry with the Rh atom located at the central site (Figure 1) was optimized. However, the $D_{\infty h}$ isomer is less stable than the quartet $C_{\infty v}$ isomer.

After the geometry of the unstable Rh-centered C_{3v} isomer is relaxed to be the C_{2v} symmetry, the doublet and quartet C_{2v} isomers are optimized to be the stable structures while the sextet C_{2v} isomer converges to be the stable C_s isomer during the geometry optimization. As seen from Figure 1, the sextet C_s isomer is analogous to the C_{2v} isomer in geometry, however, the C_s isomer with the same spin state is lower by about 0.14 hartree in total energy than the C_{2v} isomer.

As for the kitelike C_{2v}(a) RhC_4 structure, it was found that the terminal carbon atoms are attached to the C ring with the rhodium atom embedded. Like the C_{2v}(a) isomer, the total energy of the fanlike C_s(a) isomer increases monotonically, together with a drop of stability, when the spin increases from S = 1/2, to 5/2. It should be mentioned that the fanlike C_s(a) RhC_4 geometry is lower in total energy than the $D_{\infty h}$, C_{2v}, C_{2v}(a), and C_s isomers. However, it is higher by about 0.01 hartree in total energy than the $C_{\infty v}$ isomer with the same spin state. Finally, the stable scooplike C_1 isomer, which is described as a distortion of the C_{2v}(a) RhC_4 isomer above, was considered. We found that its total energy is slightly higher than those of the C_s(a) and $C_{\infty v}$ RhC_4 clusters.

On the basis of the calculated total energies of the RhC_4 isomers, the linear RhC_4 ($C_{\infty v}$, S = 3/2) cluster is the most stable structure and its electronic ground state is $^4\Sigma$. The most stable $C_{\infty v}$ RhC_4 structure is similar to that of the PdC_4 isomer[25] and deviates strongly from those of the TMC_4 (TM = Y, Nb, La, Sc, and Cr)[26−30] clusters in geometrical structures.

3.1.5. RhC_5. Guided by the calculated results on the RhC_3 and RhC_4 clusters, the RhC_5 clusters with respective $C_{\infty v}$, C_{4v}, and C_{5v} symmetries were considered. However, the Rh-capped tetragonal bipyramidal C_{4v} isomer and the Rh-capped pentagonal pyramidal C_{5v} isomer turned out not to be stable isomers. After a slight distortion of the C_{5v} isomer, stable doublet and sextet Rh-capped C_1 RhC_5 structures were finally obtained.

Ringlike C_{2v} and kitelike C_{2v}(a) isomers were optimized to be stable geometries, whereas the quartet C_{2v} isomer corresponds to a transition state. A relaxation of the quartet C_{2v} geometry along the coordinates of the imaginary vibrational mode was carried out until a true local minimum C_1(b) isomer was reached. As seen from Figure 1, the C_1(b) geometry is analogous to the C_{2v} geometry. For the kitelike C_{2v}(a) isomer, the doublet and sextet C_{2v}(a) isomers are actually formed to be the stable states. However, the quartet isomer corresponds to a transition state.

As the most likely ground state candidate, the linear $C_{\infty v}$ structure was also optimized. The doublet $C_{\infty v}$ isomer is actually the ground state of the RhC_5 unit. In addition, a bent C_1(a) isomer, which can be viewed as the Rh atom substituted for a C atom on the center site of the linear $C_{\infty v}$ RhC_5 cluster, is also optimized. The calculated results indicate that the C_1(a) isomer is the stable geometry. However, its total energy is higher than that of the linear $C_{\infty v}$ isomer.

According to the investigated RhC_5 clusters, it is found that the Rh atom in the most stable RhC_5 isomer localizes at the terminal of the linear structure and the corresponding electronic state is $^2\Sigma$. The most stable geometry is different from those of TMC_5 (TM = Y, Nb, La, and Sc)[27−30] isomers. However, it is consistent with those of the CrC_5[26] and PdC_5[25] clusters.

3.1.6. RhC_6. On the basis of the investigations on the RhC_n (n = 2−5) clusters above, a variety of possible RhC_6 isomers with respective $C_{\infty v}$, D_{6h}, and C_{6v} symmetries as the ground state candidates were investigated. The optimized results show that the Rh-capped C_{6v} isomer and the D_{6h} isomer are the unstable structures. After an adjustment of the D_{6h} geometry, a bicyclic fused stable C_1(a) isomer, which contains a triangular C−Rh−C ring, is obtained. A cyclic stable C_1 structure was also obtained by changing the location of the Rh atom and the tailing C atom. (Figure 1, C_1). When spin goes from S = 1/2, to 3/2, and to 5/2, the total energies of the C_1 and C_1(a) isomers increase. The C_1 isomer tends to have lower total energy as compared to the C_1(a) isomer with the same spin value. Consequently, the cyclic doublet C_1 structure with electronic state of ^{2}A is more stable than the doublet C_1(a) isomer. A kitelike stable C_{2v} isomer is found. The stable doublet C_{2v} isomer is higher by about 0.07 hartree in total energy than the doublet C_1 isomer.

Two RhC_6 isomers are expected to be the most likely ground state candidates: one is a linear $C_{\infty v}$ structure; The other is a distorted linear C_1(b) isomer which can obtained by an exchange of one C atom for one Rh atom in the linear $C_{\infty v}$ structure; The calculated results show that the $C_{\infty v}$ and C_1(b) RhC_6 isomers are the stable structures. In analoge to the $C_{\infty v}$ RhC_4 isomer, it is surprisingly found that the slight deviated linear doublet C_1-(b) RhC_6 isomer is higher by about 0.06 hartree in total energy than the linear quartet $C_{\infty v}$ isomer, the quartet $C_{\infty v}$ isomer is lower in total energy than the doublet and sextet isomers. Thus, the linear quartet $C_{\infty v}$ isomer is the most stable structure with electronic state of $^4\Sigma$. The Rh atom in the lowest-energy RhC_6 geometry occupies the terminal site and Rh acts as only an impurity atom for the carbon chain. It should be pointed out that the equilibrium geometry of the most stable $C_{\infty v}$ RhC_6 cluster is similar to those of the TMC_6 (TM= Cr, Y, Pd, and Nb)[25−27,30] clusters.

The available experimental data indicate that the linear pure carbon C_n chains with $2 \le n \le 9$ are the most stable structures.[54] As far as the RhC_n clusters are concerned, the linear isomer with the Rh atom acting as the terminal is the lowest-energy form for each unit of the RhC_n ($n \le 1-6$) series. The terminal Rh in the linear chain structure does not directly bind with all carbon atoms and acts as only an impurity atom without changing the framework of the most stable C_n structure. Moreover, the electronic ground state of RhC_n clusters has a

TABLE 3: Natural Populations and Natural Electron Configurations of the Most Stable RhC_n ($n = 1-6$) Clusters

system	symmetry	spin	atom	natural population	natural electron configuration
RhC	$C_{\infty v}$	1/2	Rh	−0.1379	$[core]5s^{0.69}4d^{8.45}5p^{0.01}$
			C	0.1379	$[core]2s^{1.89}2p^{1.96}3s^{0.01}$
RhC_2	$C_{\infty v}$	3/2	Rh	0.4099	$[core]5s^{0.35}4d^{8.26}$
			C(1)	−0.4007	$[core]2s^{1.34}2p^{3.03}3s^{0.02}3p^{0.02}$
			C(2)	−0.0092	$[core]2s^{1.63}2p^{2.35}3s^{0.02}3p^{0.01}$
RhC_3	$C_{\infty v}$	1/2	Rh	0.2392	$[core]5s^{0.31}4d^{8.47}$
			C(1)	0.1316	$[core]\ 2s^{1.27}2p^{2.58}3s^{0.01}3p^{0.01}$
			C(2)	−0.5211	$[core]\ 2s^{1.27}2p^{2.58}3s^{0.01}3p^{0.01}$
			C(3)	0.1504	$[core]2s^{1.62}2p^{2.22}3s^{0.01}3p^{0.01}$
RhC_4	$C_{\infty v}$	3/2	Rh	0.3914	$[core]5s^{0.28}4d^{8.34}$
			C(1)	−0.1422	$[core]2s^{1.25}2p^{2.87}3s^{0.01}3p^{0.01}$
			C(2)	−0.0454	$[core]2s^{0.94}2p^{3.09}3p^{0.01}$
			C(3)	−0.2770	$[core]2s^{0.99}2p^{3.28}3p^{0.02}$
			C(4)	0.0732	$[core]2s^{1.63}2p^{2.28}3s^{0.01}3p^{0.01}$
RhC_5	$C_{\infty v}$	1/2	Rh	0.2572	$[core]5s^{0.30}4d^{8.46}$
			C(1)	0.0595	$[core]2s^{1.27}2p^{2.66}3s^{0.01}3p^{0.01}$
			C(2)	−0.2615	$[core]2s^{0.91}2p^{3.34}3p^{0.01}$
			C(3)	0.2615	$[core]2s^{0.92}2p^{2.86}3p^{0.01}$
			C(4)	−0.3949	$[core]2s^{0.98}2p^{3.32}3p^{0.02}$
			C(5)	0.1233	$[core]2s^{1.62}2p^{2.25}3s^{0.01}3p^{0.01}$
RhC_6	$C_{\infty v}$	3/2	Rh	0.3652	$[core]5S^{0.28}4d^{8.36}5p^{0.01}$
			C(1)	−0.1102	$[core]2S^{1.26}2p^{2.83}3S^{0.01}3p^{0.01}$
			C(2)	−0.1068	$[core]2S^{0.92}2p^{3.17}3p^{0.01}$
			C(3)	−0.0094	$[core]2S^{0.89}2p^{3.11}3p^{0.01}$
			C(4)	0.0901	$[core]2S^{0.90}2p^{3.00}3p^{0.01}$
			C(5)	−0.3094	$[core]2S^{0.97}2p^{3.32}3p^{0.02}$
			C(6)	0.0805	$[core]2S^{1.63}2p^{2.28}3S^{0.01}3p^{0.01}$

TABLE 4: HOMO−LUMO Gap of the Most Stable RhC_n Clusters (unit: Hartree)

system	symmetry	spin	α-HOMO	α-LUMO	β-HOMO	β-LUMO	gap (eV)
RhC	$C_{\infty v}$	1/2	−0.19193	−0.09815	−0.24543	−0.11965	1.96602
RhC_2	$C_{\infty v}$	3/2	−0.24724	−0.10300	−0.24698	−0.15865	2.40258
RhC_3	$C_{\infty v}$	1/2	−0.24768	−0.12028	−0.23793	−0.14476	2.53422
RhC_4	$C_{\infty v}$	3/2	−0.25134	−0.10697	−0.24342	−0.16633	2.09685
RhC_5	$C_{\infty v}$	1/2	−0.25096	−0.13944	−0.23780	−0.14564	2.50675
RhC_6	$C_{\infty v}$	3/2	−0.24234	−0.10555	−0.24116	−0.17140	1.89747

strong odd−even alternation as a function of the number of carbon atoms: the doublet isomers with electronic state of $^2\Sigma$ are associated with *n*-odd members of series while the quartet isomers with electronic state of $^4\Sigma$ are associated with the *n*-even members. This even−odd effect is similar to those occurring in the C_n,[54] PdC_n,[25] CaC_n,[14] NbC_n,[29] and Zr_n[55] clusters.

3.2. Binding Energies and Fragmentation Energies. To predict the relative stability of the most stable RhC_n ($n = 1-6$) clusters, it is significant to calculate the averaged atomic binding energies ($E_b(n)$) with respect to the isolated atoms and fragmentation energies ($D(n, n-1)$) with respect to removal of one C atom from the RhC*n* clusters. The averaged atomic binding energies and fragmentation energies of the RhC_n ($n = 1-6$) clusters are defined as[45]

$$E_b(n) = \frac{nE_T(C) + E_T(Rh) - E_T(RhC_n)}{n+1}$$

$$D(n, n-1) = E_T(RhC_{n-1}) + E_T(C) - E_T(RhC_n)$$

Where $E_T(RhC_{n-1})$, $E_T(C)$, $E_T(Rh)$, and $E_T(RhC_n)$ represent the total energies of the most stable RhC_{n-1}, C, Rh, and RhC_n clusters, respectively.

The calculated results are plotted in Figure 2. Curve a in Figure 2 shows the size dependence of the average atomic binding energies ($E_b(n)$) of RhC_n clusters; curve b in Figure 2 shows the size dependence of the fragmentation energies $D(n, n-1)$ of RhC_n clusters. The features of the size evolution are obviously displayed, and the peaks of the curves correspond to those clusters having enhanced relative stabilities. It can be seen from curve a that the average atomic binding energies generally fall as the number of carbon atoms increases from $n = 1$ to $n = 2$. Thereafter, the average atomic binding energies of the clusters begin to increase with increasing *n*. This regularity is in good agreement with the observed regularity of the $IrSi_n$ ($n = 2-6$) clusters.[40] According to the calculated fragmentation energies shown in curve b, three marked peaks are found respectively at $n = 1$, $n = 3$, and $n = 5$; indicating that the corresponding clusters have enhanced stabilities and have high abundances in mass spectrum as compared to the corresponding neighbors. Consequently, the RhC_n clusters with odd-numbers of carbon atoms are relatively more stable than the neighboring ones with even-numbers of carbon atoms. The general behavior of the RhC_n clusters is very similar to that of the C_n[54] and ScC_n[30] clusters; however, it is opposite to that of PbC_n,[25] CaC_n,[14] and MgC_n[11] clusters.

3.3. Population Analyses. Our calculated results of Mulliken atomic net population on RhC_n ($n = 1-6$) clusters obtained at the B3LYP/LanL2DZ level are summarized at Table 2. We find that the Mulliken atomic net population of Rh in the most stable RhC_n ($n = 1-6$) clusters is positive, and that the nearest neighbor C of the Rh atom is negative (except in RhC_3) is in good agreement with what is found in NbC_n ($n = 3-8$),[29] YC_n ($n = 2-6$),[27] and LaC_n ($n = 2-6$)[28] clusters.

Mulliken populations were sometimes found to be misleading for $TMSi_n$ clusters,[56] whereas natural populations and natural electron configurations are a reasonable explanation of the charge transfer within the clusters.[40,45,57] For this reason, we calculated the natural population and natural electron configurations are listed in Table 3 for the RhC_n ($n = 1-6$) clusters.

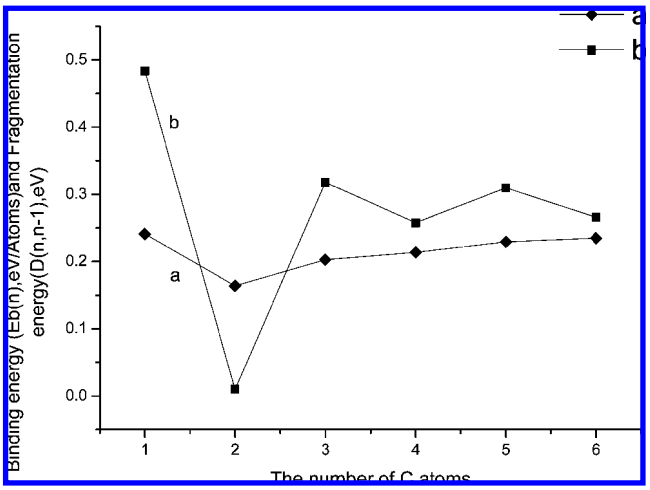

Figure 2. Size dependence of the average atomic binding energies and the fragmentation energies of the most stable RhC_n clusters.

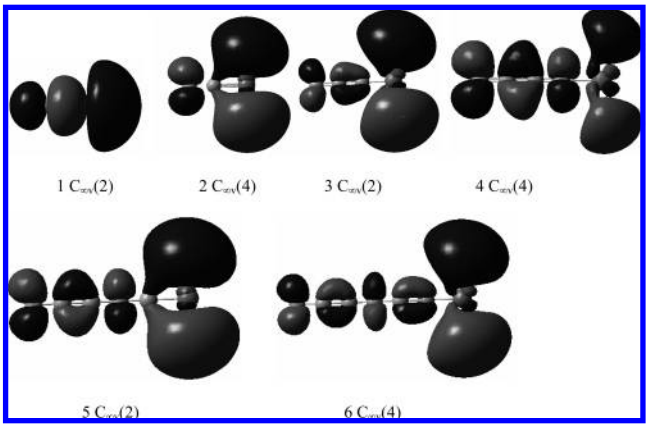

Figure 3. Contour maps of the HOMOs of the most stable RhC_n clusters; For example, the 6 $C_{\infty v}(4)$ represents the most stable quartet RhC_n cluster.

From Table 3, one finds that the natural population of the Rh atom for RhC is negative, and that it is positive for the stable RhC_n ($n = 2-6$) clusters. On the basis of the calculated natural electron configurations, we show that more than 8.3 electrons occupy the 4d subshell of Rh in the RhC_n clusters, and that the 4d orbitals of the Rh atom in RhC_n clusters do not behave as core orbitals but take an active role in chemical bonding. The charges in the RhC_n ($n = 2-6$) clusters mainly transfer from the 5s orbitals of the Rh atom and the 2s orbitals of the C atoms to the 4d orbitals of the Rh atom and the 2p orbitals of the C atoms. Consequently, the Rh atom in the most stable RhC_n clusters acts as an electron acceptor, influencing the chemical bonding properties of the C_n framework. Natural population of Rh atom in the RhC_n($n = 1-6$) units also varies with the n: the natural populations decrease with n in even-n clusters, whereas the natural populations increase with n in odd-n clusters.

3.4 HOMO−LUMO Gap. The electronic properties of RhC_n clusters are characterized by the energy gap between the highest occupied molecular orbital(HOMO) and the lowest unoccupied molecular orbital(LUMO). The calculated HOMO−LUMO gaps of RhC_n clusters are listed in Table 4. The calculated results indicate that the HOMO−LUMO gaps of RhC_3 (2.53 eV) and RhC_5 (2.51 eV) clusters are bigger than those of the other RhC_n clusters. Therefore, the chemical stabilities of these two clusters are improved dramatically as compared to the others, and the clusters with odd numbers of carbon atoms are more stable than those with even-numbers of carbon atoms. These findings are in good agreement with those of the calculated fragmentation energies above.

3.5. Chemical Bonding Properties. As seen from the HOMO of RhC_n clusters (Figure 3), the σ-type bond of RhC dimer is formed between the Rh and C atoms. However, when one Rh atom is capped on the C_2 molecule, the σ-type bond between Rh and C atoms is changed to be the π-type bond. As observed from the HOMO of RhC_3 isomer, the π-type orbitals extend over the 2C and 3C atoms (The order of carbon atoms is named from left to right). However, the shape of the HOMO and bonding property for the most stable RhC_3 cluster are obviously different from those of RhC_2 cluster. For the RhC_4, its HOMO obviously corresponds to a $\pi-$type bond between the 2C and 3C atoms, the Rh and 4C atoms formed the weak delocalized π-type bond, which is similar to that of RhC_2 cluster. However, for the RhC_5, its HOMO corresponds to the delocalized π-type bonds on 2C−3C and Rh−5C bonds. As far as the RhC_6 isomer is concerned, the 2C−3C and 5C−6C bonds are π-type bonds; The 1C, 4C, and Rh atoms appear the localized π-type bonds.

4. Conclusions

The RhC_n ($n = 1-6$) clusters with different spin states have been studied employing the B3LYP method with the Lan2DZ basis sets. The total energies, equilibrium geometries, and stabilities of RhC_n ($n = 1-6$) clusters, together with fragmentation energies and averaged atomic binding energies, were presented and discussed.

According to the calculated results, we find that the most stable Rh-terminated linear RhC_n ($n = 1-6$) geometries are similar to those of the ground states of the C_{n+1} frameworks. Therefore, linear structures are the most interesting possible targets for an experimental search of rhodium-doped carbon clusters. Furthermore, the electronic ground state has a strong even−odd alternation: the n-odd RhC_n clusters have a doublet ground state ($^2\Sigma$), whereas the n-even isomers have a quartet ground state ($^4\Sigma$). This feature is also found in C_n,[54] PdC_n,[25] CaC_n,[14] and NbC_n[29] clusters.

The relative stability of the different clusters has been discussed in term of the calculated average atomic binding energies and fragmentation energies. The calculated results exhibit an even−odd alternation trend in the cluster's stability: the n-odd RhC_n clusters are more stable than the corresponding $n - 1$ and $n + 1$ ones. The relative stability of the RhC_n ($n = 1-6$) clusters agrees with findings for C_n[54] and ScC_n[30] clusters, but it is opposite to what is found for PbC_n,[25] CaC_n,[14] and MgC_n[11] clusters.

The population analysis indicates that the charges in the RhC_n ($n = 2-6$) clusters mainly transfer from the 5s orbitals of Rh atom and the 2s orbitals of C atoms to the 4d orbitals of Rh atom and the 2p orbitals of C atoms. The Rh atom in the most stable RhC_n clusters acts as an electron absorber. Generally, the charges are transferred from the Rh atom to the C_n in the most stable RhC_n ($n = 1-6$) clusters.

Finally, the HOMO−LUMO gaps exhibit size and species dependence. These findings are in good agreement with those of the calculated fragmentation energy. In addition, the chemical bonding properties of RhC_n clusters is also discussed in this article.

Acknowledgment. This work is supported by National Fund (985−2), the HP computational center of National Sychrotron Radiation Laboratory of USTC.

References and Notes

(1) Weltner, W., Jr.; Van, R. J. *Chem. Rev.* **1989**, *89*, 1713.
(2) Raghavachari, K.; Binkley, J. S. *J. Chem. Phys.* **1987**, *87*, 2191.

(3) Kroto, H. W.; Heath, J. R.; O Brien, S. C.; Curl, R. F.; Smalley, R. E. *Nature* **1985**, *318*, 162.
(4) Williams, D. A. *Molecules and Grains in Space*; Proceedings of the 50th International Meeting of Physical Chemistry, Mont Sainte-Odile, France, Sept 1993; Nenner, I., Ed.; AIP Conference Proceedings No. 312; American Insitute of Physics: Melville, NY, 1994.
(5) Lee, S. *Chem. Phys. Lett.* **1997**, *268*, 69.
(6) Fye, J. L.; Jarrold, M. F. *J. Phys. Chem. A* **1997**, *101*, 1836.
(7) Pascoli, G.; Lavendy, H. *J. Phys. Chem. A* **1999**, *103*, 3518.
(8) Largo, A.; Cimas, A.; Redondo, P.; Barrientos, C. *Int. J. Quantum Chem.* **2001**, *84*, 127.
(9) Largo, A.; Redondo, P.; Barrientos, C. *J. Phys. Chem. A* **2002**,*106*, 4217.
(10) Redondo, P.; Barrientos, C.; Largo, A. *Int. J. Quamtum Chem.* **2004**, *96*, 615.
(11) Redondo, P.; Barrientos, C.; Cimas, A.; Largo, A. *J. Phys. Chem. A* **2003**, *107*, 4676.
(12) Redondo, P.; Barrientos, C.; Cimas, A.; Largo, A. *J. Phys. Chem. A* **2003**, *107*, 6317.
(13) Largo, A.; Redondo, P.; Barrientos, C. *J. Phys. Chem. A* **2004**, *108*, 6421.
(14) Redondo, P.; Barrientos, C.; Largo, A. *J. Phys. Chem. A* **2004**, *108*, 11132.
(15) Rohmer, M.; Benard, M.; Poblet, J.-M. *Chem. Rev.* **2000**, *100*, 495.
(16) Pelino, M.; Haque, R.; Bencivenni, L.; Gingerich, K. A. *J. Chem. Phys.* **1988**, *88*, 6534.
(17) Clemmer, D. E.; Shelimov, K. B.; Jarrold, M. F. *Nature* **1994**, *367*, 718.
(18) Yeh, C. S.; Byun, Y. G.; Afzaal, S.; Kan, S. Z.; Lee, S.; Freiser, B. S.; Hay, P. J. *J. Am. Chem. Soc.* **1995**, *117*, 4042.
(19) Simard, B.; Presunka, P. I.; Loock, H. P.; Berces, A.; Launila, O. *J. Chem. Phys.* **1997**, *107*, 307.
(20) Li, X.; Liu, S. S.; Chen, W.; Wang, L. S. *J. Chem. Phys.* **1999**, *111*, 2464.
(21) Langenberg, J. D.; Shao, L.; Morse, M. D. *J. Chem. Phys.* **1999**, *111*, 4077.
(22) Li, X.; Wang, L. S. *J. Chem. Phys.* **1998**, *109*, 5264.
(23) Hamrick, Y. M.; Weltner, W., Jr. *J. Chem. Phys.* **1991**, *94*, 3371.
(24) Van Zee, R. J.; Bianchini, J. J.; Weltner, W., Jr. *Chem. Phys. Lett.***1986**, *127*, 314.
(25) Li, G.; Xing, X.; Tang, Z. *J. Chem. Phys.* **2004**, *118*, 6884.
(26) Zhai, H. J.; Wang, L. S.; Jena, P.; Gutsev, G. L.; Bauschlicher, C. W., Jr. *J. Chem. Phys.* **2004**, *120*, 8996.
(27) Strout, D. L.; Hall, M. B. *J. Phys. Chem.* **1996**, *100*, 18007.
(28) Roszak, S.; Balasubramanian, K. *J. Chem. Phys.* **1997**, *106*, 158.
(29) Dai, D.; Roszak, S.; Balasubramanian, K. *J. Phys. Chem. A* **2000**, *104*, 9760.
(30) Redondo, P.; Barrientos, C.; Largo, A. *J. Phys. Chem. A* **2006**, *110*, 4057.
(31) Han, H.; Liao, M.; Balasybramanian, K. *Chem. Phys. lett.* **1997**, *280*, 423.
(32) Shim, I.; Mandix, K.; Gingerich, K A. *TheoChem* **1997**, *393*, 127.
(33) Han, J. G.; Sheng, L. S.; Zhang, Y. W.; Morales, J. A. *Chem. Phys.* **2003**, *294*, 211.
(34) (a)McKee, M. L.; Woreley, S. D. *J. Phys. Chem.* **1988**, *92*, 3699. (b)McKee, M. L.; Dai, C. H.; Woley, S. D. *J. Phys. Chem.* **1988**, *93*, 3989.
(35) Becke, A. D. *J. Chem. Phys.* **1993**, *98*, 1372.
(36) Lee, C.; Yang, W.; Parr, R. G. *Phys. Rev. B.* **1998**, *27*, 785.
(37) Handy, N. C.; Schaefer, III, H. F. *J. Chem. Phys.* **1984**, *81*, 5031.
(38) Wardt, W. R.; Hay, P. J. *J. Chem. Phys.* **1985**, *82*, 284.
(39) Nicklass, A.; Dolg, M.; Stoll, H.; Preuss, H. *J. Chem. Phys.* **1995**, *102*, 8942.
(40) Han, J. G. *Chem. Phys.* **286**, *181*, 2003.
(41) Martin, L.; Ei-Yazal, J. M.; Francois, J. P. *Chem. Phys. Lett.* **1995**, *242*, 570.
(42) Mains, G. J.; White, J. M. *J. Phys. Chem.* **1991**, *95*, 112.
(43) Majumdar, D.; Balasubramanian, K. *Chem. Phys. Lett.* **1998**, *284*, 273.
(44) Barnes, M.; Merer, A. J.; Metha, G. F. *J. Chem. Phys.* **1995**, *103*, 8360.
(45) Han, J. G.; Zhao, R. N.; Duan, Y. H. *J. Phys. Chem. A.* **2007**, *111*, 2148.
(46) Kalemos, A.; Mavridis, A.; Harrison, J. F. *J. Phys. Chem. A* **2001**, *105*, 755.
(47) Denis, P. A.; Balasubramanian, K. *J. Chem. Phys.* **2005**, *123*, 054318.
(48) Li, G. L.; Tang, Z .C. *J. Phys. Chem. A* **2003**, *107*, 5317.
(49) Shim. I.; Gingerich, K. *J. Chem. Phys.* **1984**, *81*, 5937.
(50) Norman, J. G.; Kolari, H. J. *J. Am. Chem. Soc.* **1978**, *100*, 791.
(51) Hendrickx, M. A.; Clima, S. *Chem. Phys. Lett.* **2004**, *388*, 284.
(52) Barrientos, C.; Redondo, P.; Largo, A. *Chem. Phys. Lett.* **2000**, *320*, 481.
(53) Barrientos, C.; Redondo, P.; Largo, A. *Chem. Phys. Lett.* **2001**, *343*, 563.
(54) Yang, S.; Taylor, K. J.; Craycraft, M. J.; Conceico, J.; Pettiette, C. I.; Cheshnovsky, O.; Smalley, R. E. *Chem. Phys. Lett.* **1988**, *144*, 431.
(55) Wang, C. C.; Zhao, R. N.; Han, J. G. *J. Chem. Phys.* **2006**, *124*, 194301.
(56) Han, J. G.; Shi, Y. Y. *Chem. Phys.* **2001**, *266*, 33.
(57) Wang, J.; Han, J. G. *Chem. Phys.* **2007**, *342*, 253.